Pharm Res (2014) 31:2479–2489
DOI 10.1007/s11095-014-1344-0

RESEARCH PAPER

Characterization and Evaluation of Multi-Component Crystals of Hydrochlorothiazide

Renu Chadha • Swati Bhandari • Sadhika Khullar • Sanjay K. Mandal • D. V. S. Jain

Received: 18 October 2013 / Accepted: 24 February 2014 / Published online: 22 April 2014

ABSTRACT

Purpose The present work aims at improving the physicochemical properties of hydrochlorothiazide, a poorly water soluble antihypertensive drug by preparing its multi-component crystals with nicotinic acid (HCT-NA) and 2-picolinic acid (HCT-PIC).

Methods The crystals prepared by solution crystallization were investigated by thermoanalytical techniques. The crystal structures of HCT-NA (**1**) and HCT-PIC (**2**) were determined by the single crystal X-ray diffraction and were assessed for their aqueous solubility, antihypertensive activity and acute toxicity in rats.

Results Both **1** and **2** crystallized in the orthorhombic space group $P2_12_12_1$ and formation of salts were confirmed. The solubility profiles of **1** and **2** in basic media showed a maximum release of 2.5 mg/ml and 1.9 mg/ml, respectively, in comparison to the drug (0.82 mg/ml). The *in-vivo* antihypertensive activity of **1** in deoxycorticosterone acetate salt induced hypertensive rats showed 1.5 fold improvement. No increase in the signs of toxicity were revealed in rats during the acute toxicity studies even at doses of 2,000 mg/kg by body weight in comparison to the free drug. Histopathological findings supported the safety of these multi-component crystals.

Conclusions The new solid phases exhibit potential to be explored for the oral drug delivery of HCT with improved solubility and therapeutic outcome.

KEY WORDS acute toxicity · antihypertensive activity · multi-component crystals · poorly water soluble drugs · solubility

ABBREVIATIONS

ANOVA	One way analysis of variance
CMC	Sodium carboxymethyl cellulose
DSC	Differential Scanning Calorimetry
FT-IR	Fourier Transform Infrared Spectroscopy
h	Hours
HCT	Hydrochlorothiazide
HCT-NA	Salt of hydrochlorothiazide with nicotinic acid
HCT-PIC	Salt of hydrochlorothiazide with 2-picolinic acid
HPLC	High Performance Liquid Chromatography analysis
M	Mean
min	Minutes
OECD	Economic Co-operation and Development
PXRD	Powder X-ray Diffraction
SCXRD	Single crystal X-ray diffraction
SD	Standard deviation
TGA	Thermogravimetric Analysis

INTRODUCTION

Poor aqueous solubility posing one of the greatest challenges during development of innovative drugs emerging from the drug discovery programs, stand to benefit from changes in crystal structure (1,2). The solubility of crystal forms and the dissolution rate of the orally delivered APIs critically impacts their pharmacokinetic profile. (3–6) Formulation scientists often turn to various approaches, such as salt formation (7), complexation (8), co-crystallization (9) and amorphization (10,11) in order to improve the solubility and the dissolution rate of the poorly water soluble APIs. Investigation of crystal polymorphism, which is dependant on the conformational flexibility and packing arrangement of molecules may also be advantageous in optimization of the physical properties of a pharmaceutical solid (12,13).

Electronic supplementary material The online version of this article (doi:10.1007/s11095-014-1344-0) contains supplementary material, which is available to authorized users.

R. Chadha (✉) · S. Bhandari
University Institute of Pharmaceutical Sciences, Panjab University
Chandigarh 160014, India
e-mail: renukchadha@rediffmail.com

S. Khullar · S. K. Mandal (✉)
Department of Chemical Sciences
Indian Institute of Science Education and Research, Mohali
Sector 81, Manauli PO, S.A.S. Nagar
Punjab 140306, India
e-mail: sanjaymandal@iisermohali.ac.in

D. V. S. Jain
Department of Chemistry Panjab University, Chandigarh 160014, India

Hydrochlorothiazide (HCT), a thiazide diuretic used in the treatment of hypertension exhibits poor water solubility (0.7 mg/ml) as well as low permeability (logP = −0.15) (14) that hamper its potential beneficial effects. Formation of multi-component crystals (co-crystals, salts and solvates) is one of the important strategies to improve its biopharmaceutical properties in its pure form. Reports are available on the existence of polymorphs (15,16), solvates and cocrystals of HCT. However, among the two anhydrous forms (form I and form II), form II is more water soluble and is not commercially available due to its unstable nature. Furthermore, the toxic nature of the reported solvates of HCT with dioxane, DMSO, methyl acetate, N-methyl pyrollidone, DMA and aniline (17) limits their utility in a formulation. Cocrystals of HCT (18) with 18-crown-6, piperazine and nicotinic acid are patented but no solubility or *in vivo* studies are reported. The present work explores the potential of new salts of hydrochlorothiazide with nicotinic acid (HCT-NA) and 2-picolinic acid (HCT-PIC) to improve the solubility and antihypertensive efficacy of this poorly water soluble API.

Both the salts, HCT-NA (**1**) and HCT-PIC (**2**) have been structurally characterized by single crystal X-ray diffraction. In order to carry out the toxicological evaluation, the acute oral toxicity studies of (**1**) have also been performed in accordance to the Organisation for Economic Co-operation and Development (OECD) guideline number 425 and the LD50 of (**1**) has been established (19). Histopathology of the vital organs of treated animals provided direct evidence for its safety.

MATERIALS AND METHODS

Materials

The anhydrous crystalline form of hydrochlorothiazide (99.69% purity, 60–100 μm) was obtained as a gift sample from Biochem Pharmaceutical Industries Ltd, Mumbai, India. HPLC grade acetonitrile was purchased from Merck. All other solvents were of AR grade. Nicotinic acid (99.5% purity) and 2-picolinic acid (99.0% purity) were purchased from Himedia.

Sample Preparation

HCT-Form I

To obtain the single crystals of HCT (form I), a saturated solution of a commercial sample was prepared in a 1:4 mixture of THF and water and was allowed to evaporate slowly at room temperature. Crystals suitable for single crystal X-ray diffraction analysis (a typical size of 0.3 mm × 0.3 mm × 0.3 mm) were obtained after 3 days. The crystals were filtered, dried and stored in air tight glass vials.

HCT-NA (1)

148.8 mg of HCT (0.5 mmoles) were dissolved in 10 mL of methanol presaturated with nicotinic acid and allowed to evaporate slowly at room temperature. Crystals suitable for single-crystal X-ray diffraction analysis obtained in 4–5 h were filtered and dried under vacuum at 30°C for 2 days and stored in glass vials.

HCT-PIC (2)

123.1 mg (1 mmole) of 2-picolinic acid were dissolved in 12 mL of acetonitrile. To this solution, 148.8 mg HCT (0.5 mmol) were slowly added, dissolved and allowed to evaporate at room temperature. Crystals suitable for single-crystal X-ray diffraction analysis obtained in 10–12 h were filtered and dried under vacuum at 30°C for 2 days and stored in glass vials (*vide infra*).

Powder X-ray Diffraction (PXRD)

PXRD patterns were collected on X'Pert PRO diffractometer system (Panalytical, Netherlands) with a Cu Kα radiation (1.54060 Å). The tube voltage and current were set at 45 kV and 40 mA respectively. The divergence slit and anti-scattering slit settings were set at 0.48° for the diffraction experiment on the 10 mm sample size. Each sample was placed in an aluminium sample holder and measured by a continuous scan between 5° and 50° in 2θ with a step size of 0.017° and a step time of 25 s/step.

Differential Scanning Calorimetry (DSC)

Thermal analyses of the samples were performed on a DSC Q20 (TA Instruments, USA) which was calibrated for temperature and heat flow accuracy using indium (mp: 156.6°C and ΔH:25.45 J g^{-1}). The samples (3–5 mg) were placed in sealed non-hermetic aluminum pans and were scanned at a heating rate of 10°C/min from 30 to 300°C under a dry nitrogen atmosphere with a flow rate of 50 cc/min.

Thermogravimetric Analysis (TGA)

TGA was performed on a Mettler Toledo TGA/SDTA 851c instrument. Approximately 5 mg sample was heated from 30 to 300°C in open alumina pan at the rate of 10°C/min under nitrogen purge with a flow rate of 50 cc/min.

Fourier Transform Infrared Spectroscopy (FT-IR)

A Spectrum RX I FT-IR spectrometer (Perkin Elmer, UK) was employed in the diffuse-reflectance mode for collection of data. Dry KBr (20 mg) was finely ground in an agate mortar

and mixed gently with the 2 mg of the sample. A manual press was used to form the pellet. The number of scans were 32 and a resolution was 4 cm^{-1}. The data were collected over the range of 4,000-400 cm^{-1} and analyzed using Spectrum software.

Single Crystal X-ray Diffraction (SCXRD)

X-ray diffraction data sets were collected on a Bruker AXS Kappa APEX II diffractometer equipped with a CCD detector (with the crystal-to-detector distance fixed at 60 mm) using sealed-tube monochromated Mo-Kα radiation (0.71073 Å) at room temperature (296 K). The crystal centering, unit cell determination, refinement of the cell parameters and data collection was controlled through the program APEX2 (20). The frames were integrated with the Bruker SAINT software package using a narrow-frame algorithm. Data were corrected for absorption effects using the multi-scan method (SADABS) (20). The structure was solved by direct methods using SHELXS-97 and refined against F^2 using SHELXL-97 (21). All calculations were performed using the SHELXTL V 11.0 suite of programs. (22) There were no residual peaks for all structures > 1e/Å^3. All hydrogen atoms were placed in ideal positions and refined as riding atoms with individual isotropic displacement parameters. Crystallographic parameters and basic information pertaining to data collection and structure refinement for all compounds are summarized in Table I. All figures were drawn using Mercury V 3.0 (22) and hydrogen bonding parameters were generated using PLATON (23). The final positional and thermal parameters of the non-hydrogen atoms for all structures are listed in the CIF files. Crystallographic data (excluding structure factors) for the structures in this paper have been deposited with the Cambridge Crystallographic Data Centre as supplementary publication no. CCDC 961962-961963.[1]

High Performance Liquid Chromatography Analysis

The concentration of the HCT solution was determined by a Waters Alliance HPLC system which includes a Waters 2695 separation module, a Waters 2996 Photodiode Array Detector and a 4.6 mm × 150 mm SunFire™ C18, 5 µm column (Waters Corporation, Milford, MA).

Stock standards of HCT for solubility and dissolution studies were prepared by dissolving HCT in methanol and dilution with the mobile phase. Mobile phase consisting of a mixture of 0.05 M phosphate buffer (pH 3.0) and ACN (80:20) was used to prepare various concentrations of calibration standards in a range of 1–10 µg/mL. The samples of the solubility experiment were diluted with the mobile phase and injected (20 µL) onto the column in triplicate. The mobile phase was pumped at a flow rate of 0.8 mL/min through the column at a temperature of 30°C. HCT was detected at 272 nm.

Solubility Studies

The equilibrium solubility of the drug, HCT-NA and HCT-PIC were performed in distilled water ($n=3$) by adding an excess amount of solid phase (about 30 mg) to 25 ml of media pre-equilibrated at 37°C contained in a flask. The resulting slurry was shaken in a water bath shaker at 120 rpm. Aliquots of the slurries were taken at 24 h.

The solubility profiles of the drug and the prepared phases were also determined in phosphate buffer pH 7.4 to mimic the gastrointestinal tract conditions at various time intervals (5 min, 10 min, 20 min, 30 min, 45 min, 60 min, 120 min, 240 min, 360 min).

Samples were filtered through a 0.45 µm nylon filter and assayed for the drug content using HPLC at 272 nm. The residual solids after the 24 h experiment were analysed by FT-IR spectroscopy.

In Vivo Pharmacodynamic Activity

Preparation and Administration of Doses

HCT, NA and **1** were passed through #60 and suspended in 0.5% (*w*/*v*) sodium carboxymethyl cellulose (CMC) with the help of a magnetic stirrer just before administration. Assay of the samples was also performed to confirm the stability in suspension form. The preparations were administered by oral gavage once daily for a period of 6 days. The animals were treated with HCT dose equivalent to 10 mg/kg BW.

Antihypertensive Activity Evaluation

Evaluation of antihypertensive activity of HCT and **1** were performed in DOCA-salt induced hypertensive rats. 4–5 weeks old female Wistar rats (200–300 g) were procured and maintained in the central animal house of Panjab University. Animals were housed (4 rats per cage) at a relative humidity of 65 ± 2%, temperature of 25 ± 2°C with a 12-h natural light/dark cycle. They were provided with standard pellet diet and water *ad libitum*. Experiments were performed as per guidelines of committee for the purpose of the CONTROL AND SUPERVISION ON EXPERIMENTS ON ANIMALS (CPCSEA). The experimental protocol was approved by Institutional Animal Ethics Committee (I.A.E.C.). After 1 week of adaptation to laboratory conditions, the animals were randomly assigned to 5 experimental groups each comprising of 6 animals ($n = 6$).

[1] Copies of the data can be obtained, free of charge, on application to CCDC, 12 Union Road, Cambridge CB2 1EZ, UK, (fax: +44-(0)1223-336033 or e-mail: deposit@ccdc.cam.ac.uk).

Table I Crystallographic Data and Structure Refinement Parameters for HCT-NA (1) and HCT-PIC (2)

Parameters	HCT-NA (**1**)	HCT-PIC (**2**)
chemical formula	$C_7H_8ClN_3O_4S_2.C_6H_5NO_2$	$C_7H_8ClN_3O_4S_2.C_6H_5NO_2$
stoichiometry	1:1	1:1
formula wt	420.85	420.85
temperature (K)	296(2)	296(2)
wavelength (Å)	0.71073	0.71073
crystal system	$P2_12_12_1$	$P2_12_12_1$
space group	orthorhombic	orthorhombic
a (Å)	7.3330(9)	7.6271(6)
b (Å)	13.2101(19)	13.1548(9)
c (Å)	16.217(2)	16.0289(10)
α (deg)	90	90
β (deg)	90	90
γ (deg)	90	90
Z	4	4
V (Å^3)	1570.9(3)	1608.23
density (g·cm^{-3})	1.775	1.73
μ(mm^{-1})	0.553	0.540
F(000)	860	856
θ range for data collection	1.99 to 25.08°	2.54 to 24.99°
reflns collected	10670	7793
independent reflns	2766	2814
reflns with $I > 2\sigma(I)$	2382	2111
R_{int}	0.0514	0.0781
no. of parameters refined	241	241
GOF on F^2	0.975	0.927
final R_1[a]/wR_2[b]($I > 2\sigma(I)$)	0.0439/0.1153	0.0532/0.1199
R_1[a]/wR_2[b] (all data)	0.0540/0.1231	0.0787/0.1370
largest diff. peak and hole (e·Å^{-3})	0.513 and −0.413	0.395 and -0.337

[a] $R_1 = \Sigma||F_o| - |F_c||/\Sigma|F_o|$.
[b] $wR_2 = [\Sigma w(F_o^2 - F_c^2)^2 / \Sigma w(F_o^2)^2]^{1/2}$, where $w = 1/[\sigma 2(F_o^2) + (aP)^2 + bP]$, $P = (F_o^2 + 2F_c^2)/3$.

Group I (Control Group). These rats were vehicle treated. Cotton seed oil (0.1 ml/100 g) was injected subcutaneously twice a week for 6 weeks and 0.5% (*w*/*v*) CMC suspension was administered by oral gavage after 6 weeks.

Group II (DOCA + 1% (w/v) NaCl-DOCA Control Group). In the second group, hypertension was induced in rats by subcutaneous injection of 15 mg/kg of DOCA dissolved in cotton seed oil, twice weekly for a 6 week period. Drinking water was replaced by 1%*w*/*v* sodium chloride solution (NaCl). The systolic blood pressure was recorded before and once weekly after the DOCA treatment. To establish the base line blood pressure recordings were made at three separate occasions. After the induction of hypertension (6 weeks) this group received a single oral dose therapy of CMC suspension for a period of 6 days.

Group III (DOCA + 1% (w/v) NaCl Followed by HCT). Similar to group II, hypertension was induced in this group and it received a single oral dose therapy of 10 mg/kg of HCT in 0.5% (*w*/*v*) CMC suspension per day (rats fasted overnight) for a period of 6 days.

Group IV (DOCA + 1% (w/v) NaCl Followed by **1***)*. Hypertension was induced in this group (similar to group II) and the hypertensive rats were treated with single oral dose therapy of **1** equivalent to 10 mg/kg HCT per day (rats fasted overnight) for 6 days.

Group V (DOCA + 1% (w/v) NaCl Followed by NA). After induction of hypertension, rats were treated with single oral dose therapy of NA equivalent to 5 mg/kg per day (rats fasted overnight) for 6 days.

Changes in systolic blood pressure of all the groups were recorded after 24 h of dose administration every day for 6 days to evaluate the antihypertensive efficacy of **1**, in comparison to groups I (control), II, III and V.

Blood Pressure Recording in Rats

The systolic blood pressure of each rat was measured at weekly intervals for 6 weeks. The rat tail was heated with 200 W bulb heat lamp for 3–5 min and blood pressure was

recorded using non-invasive blood pressure measurement technique (NIBP- Biopac-MP 100, USA). At least 3 separate indirect pressure values were averaged for each animal. The animals having systolic blood pressure ≥180 mmHg were considered as hypertensive.

Statistical Analysis

Data was expressed as mean (M) ± standard deviation (SD). One way analysis of variance (ANOVA) was used for each parameter, followed by Tukey's test. $P<0.001$ is considered statistically significant.

Acute Toxicity Studies

The acute oral toxicity study was performed in female rats as per Organisation for Economic Co-operation and Development (OECD) guideline number 425 to determine LD50 of HCT-NA in comparison to HCT and to establish the safety of (1) (see Supplementary Material). In addition, the test allows the observation of signs of toxicity (19).

Preparation and Administration of Doses for Acute Toxicity Studies

HCT and (1) were suspended in 0.5%*w*/*v* CMC and single oral doses were administered.

Animals for Acute Toxicity Studies

Healthy young adult nulliparous and nonpregnant female Wistar rats, weighing 110–120 g (10–12 weeks old, at the start of the experiment), were procured and maintained at central animal house in Panjab University, Chandigarh as described in the previous section.

Main Test

Since the LD_{50} (>2,000 mg/Kg BW) value of HCT is known, the testing directly proceeded to main test (without conducting the limit tests). All animals were on fasting overnight prior to dose administration. Using the default progression factor, doses were calculated using aot425 software after selecting LD_{50} of 2,000 mg/Kg BW/rat as the assumed LD_{50}. Initial dose (630 mg/Kg BW) was selected based on the reported LD_{50} of HCT and the subsequent doses were calculated with a dose progression factor of 3.2 (2,000 mg/Kg BW/rat).

Observations

Animals were observed during the first 30 min after dosing and periodically thereafter during the first 24 h, and once daily for a total of 14 days. Attention was given for observations of tremors, convulsions, salivation, diarrhoea, lethargy, sleep and coma. Individual weights of animals were recorded before the administration of drug on 1st day and on the 14th day of the experiment. Changes in the weight of individual animals were calculated and compared with that of the control animals.

Statistical Analysis

Changes in BW were expressed as M ± SD and their statistical significance was calculated using *t*-test. LD50 was determined using acute oral toxicity (Guideline 425) and by using statistical program (aot425, Version: 1.0).

Morphological and Pathological Examinations

The exposed rats were anesthetized, post 14 day observation by i.p. pentobarbital at 48 h and autopsied. The organs such as stomach, liver and kidney were stripped out, immediately fixed in 10% formalin and subjected to histopathological examinations. The tissues of organ samples were embedded in paraffin blocks, then sliced and placed onto glass slides. After histological H-E staining, the slides were observed and the photographs taken using optical microscope (Carl Zeiss, Axioscope A1).

RESULTS AND DISCUSSION

Multi-component crystals (**1**) and (**2**) prepared by solution crystallization method were characterized using PXRD and thermal techniques (DSC and TGA). The exact phase identification (multi-component crystal/salt) was determined by single crystal X-ray diffraction and FT-IR spectroscopy.

PXRD

The PXRD patterns for HCT, NIC, **1**, PIC and **2** are given in Fig. 1. New peaks were observed in the PXRD patterns of the prepared compounds at 2θ values of 5.8, 12.9, 6.1, 23.9 and 25.0° (1) and 8.8, 12.9, 14.7, 17.5, 17.9, 18.0, 17.5, 17.9, 18.0, 21.1, 27.1, 27.7, 28.6, 29.3, 29.5, 31.1 (2) suggesting the formation of new phases.

The experimental and the simulated PXRD patterns of **1** and **2** are compared in Figure S1. The resemblance of the two patterns in this spectrum validates the method of preparation and indicates the purity of the new phases.

DSC and TGA

DSC curves showing the thermal behavior of the HCT, NA, HCT-NA (1), PIC, HCT-PIC physical mixture and

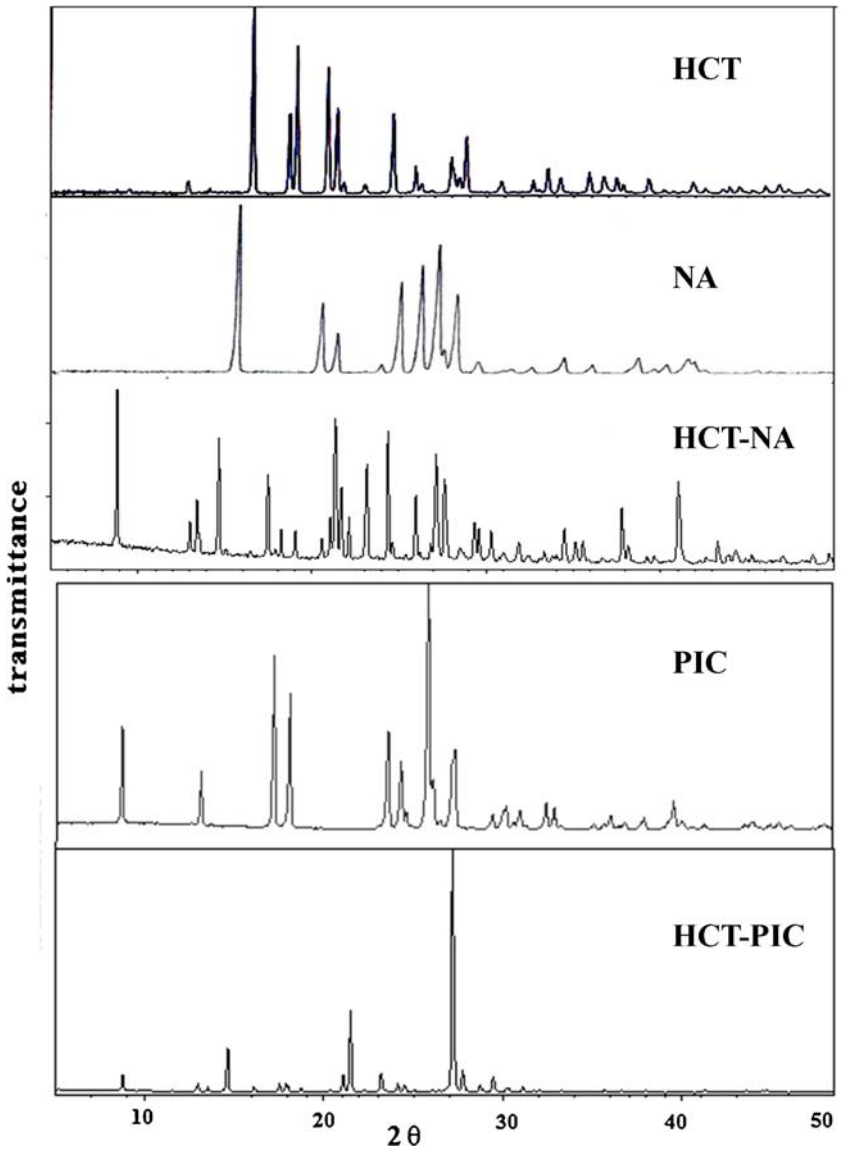

Fig. 1 PXRD patterns of HCT, NA, HCT-NA, PIC, HCT-PIC.

HCT-PIC (**2**) are shown in Figure S2. The reported temperatures are the peak temperatures. Appearance of a melting endothermic peak of HCT at 269°C indicates it to be form I (17). A single sharp endothermic peak in the DSC scan of HCT-NA at 264°C which is in between that of the drug (269°C) and the counter molecule, NA (232°C) confirms the formation of a new crystalline phase.

Similarly, in the DSC scan of HCT-PIC (2), the sharp melting endothermic event at 196°C represents the existence of a new solid phase. Subsequently, a small and broad endothermic peak associated with a weight loss of 30.8% (200–250°C) in TGA is due to decomposition of PIC immediately after the melting of HCT-PIC (2)**.** The decomposition endothermic peak is also present in the DSC scan of pure picolinic acid. The weight loss in TGA (Figure S3) correlated well with the theoretical weight loss of 29.25% corresponding to a single molecule of picolinic acid suggesting a stoichiometry of 1:1 between HCT and PIC in HCT-PIC (2).

Phase Identification

A crucial step in a multi-component molecular crystal characterization is to determine if a new compound is a multi-component crystal (an unionized species) or a salt (an ionized species). HCT is a weak base and has two pKa values of 7.9 and 9.2 corresponding to the -NH2 and –NH functionalities respectively. NA has a pKa of 2.2 for the -COOH group and 4.9 for the aromatic ring N while PIC exhibits a pKa of 1.07 for the -COOH group and 5.25 for the aromatic ring N (Scheme1). The pK_a difference between HCT and the counter molecules suggests the possibility of salt formation (24) that was

Scheme I Molecular structures of hydrochlorothiazide and the coformers used in the study.

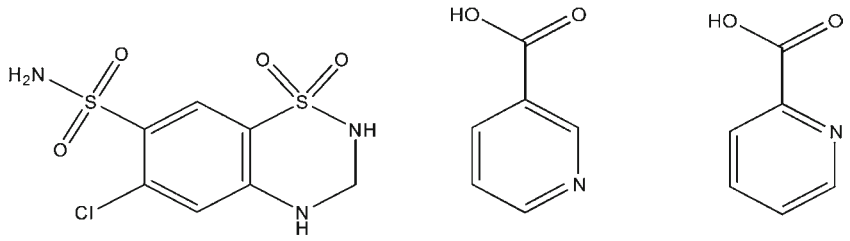

confirmed by Fourier transform infrared spectroscopy (FT-IR) and single crystal X-ray diffraction (SCXRD).

FT-IR Spectroscopy

A significant decrease in the –NH stretching frequency of HCT from 3,268 and 3,170 cm^{-1} to 3,253 and 3,159 cm^{-1} respectively and the –C = O stretching frequency of NA from 1,708 cm^{-1} to 1,647 cm^{-1} was observed in the FT-IR spectra of HCT-NA (Figure S4). Similarly, a decrease in the –C = O stretching frequency of PIC from 1,715 cm^{-1} to 1,675 cm^{-1} (in HCT-PIC) suggested the presence of ionized O atom of the carbonyl group. Furthermore, HCT-NA and HCT-PIC also showed broad bands between 3,300 and 2,000 cm^{-1} corresponding to $N–H^+$ signals of amine hydrogen bonded salts (absent in the spectrum of HCT). Thus, FT-IR spectra of the multi-component crystals imply HCT-salt formation.

SCXRD

Crystal structures of **1** and **2** were determined by single crystal X-ray diffraction studies. For direct structural comparison of the new multi-component crystals with that of HCT, suitable crystals of form I were grown and subjected to single crystal X-ray diffraction as the cif file of HCT form I was unavailable. The structural information of HCT form I[2] is similar to the reported form I of HCT (15,17).

The HCT form I crystallizes in the monoclinic space group $P2_1$. The crystal structure of HCT (form I) is stabilized by hydrogen bonded units of the drug molecules showing four dominant supramolecular synthons as shown in Fig. 2. The series of intermolecular hydrogen bonded contacts include three N–H….O contacts, one N–H….N contact, three C–H…O contacts and two intramolecular contacts involving a Cl atom.

All the hydrogen bonding parameters are listed in Table S1.

[2] Crystal Structure Data for HCT form I: formula, $C_7H_8ClN_3O_4S_2$; T = 296 (2) K; Mr = 297.73; Wavelength, Mo Kα; Crystal system and space group, Monoclinic, $P2_1$; unit cell parameters, a = 7.3822(19) Å, b = 8.459(3)Å, c = 9.958(3)Åβ = 111.700(13)°V = 577.8 (3) $Å^3$, Z = 2, μ = 0.698 mm^{-1}, Density = 1.711 Mg/cm^3, Theta max = 25.12° Reflections collected = 2217, I > 2σ(I) = 1357, S = 1.029, R = 0.0307.

The incorporation of the molecules, NA and PIC in the crystal lattice of the drug molecules breaks all the H-bonds except one, N3–H3….O2 (conserved in **2**) which was originally present in the drug molecule and introduces new N–H….O hydrogen bonded interactions. However, the C-H…O interaction (C3–H3A…O4) of the drug molecule (Fig. 2b) is conserved in both (**1**) and (**2**).

The molecular packing in Form I shows supramolecular synthons formed *via* strong N-H···O hydrogen bonds between free sulfonamide group of one HCT molecule and ring sulfonamide group of adjacent HCT molecule (N1H1…O1 (N/O 2.875(4) Å, N/H 0.88 Å, N-H/O 122°) and N2H2B…O3 (N/O 2.918(5) Å, N/H 0.88 Å, N-H/O 157°) resulting in the formation of drug dimer (Fig. 2a). Thus, HCT drug molecules are present in the form of dimeric units and each unit is linked to the adjacent dimer through N-H…O hydrogen bond (N3H3…O2, (N/O 2.915(5) Å, N/H 0.88 Å, N-H/O 147°).

HCT-NA (1) crystallizes in the orthorhombic space group $P2_12_12_1$ with the asymmetric unit consisting of one molecule of HCT and one molecule of nicotinic acid (Fig. 3). In HCT-NA, supramolecular homosynthon (N3H3/O1, N/O 2.38 Å, N/H 0.86 Å, N-H/O 125°) is involved in the formation of dimers of the HCT molecules. The HCT molecule is hydrogen bonded to nicotinic acid molecule *via* two NH…O heterosynthons (N2–H2A….O5(3.027(5)Å, N/H 0.72(5)Å, N-H/O 160(6)° and N2–H2B….O5 N/O 2.971(4) Å, N/H 0.814(4)Å, N-H/O 167(4)°). The nicotinic acid molecules form dimers through N4–H….O6 contact (N/O 2.640 Å) (This bond distance was taken from analysis of the structure by Mercury software).

Similarly, HCT-PIC (2) crystallizes in the orthorhombic $P2_12_12_1$ space group with the asymmetric unit consisting of one molecule of HCT and one molecule of picolinic acid (Fig. 4). Here, the N3—H3…O2 homosynthon (N3H3/O2, N/O 2.919(6) Å, N/H 0.86 Å, N-H/O 126°) is involved in the formation of dimers of the HCT molecules. The HCT molecule is hydrogen bonded to PIC molecule *via* supramolecular synthons, (N2H2A….O6, N/O 3.040(7) Å, N/H 0.81(7) Å, N-H/O 152(7)° and N2H2B….O6 N/O 3.119(7) Å, N/H 0.97(7) Å, N-H/O 168(5)°. Another heterosynthon N4–H….O4 (N/O 3.045 Å) is formed between the HCT and the PIC molecules. (This bond distance was taken from analysis of the structure by Mercury software).

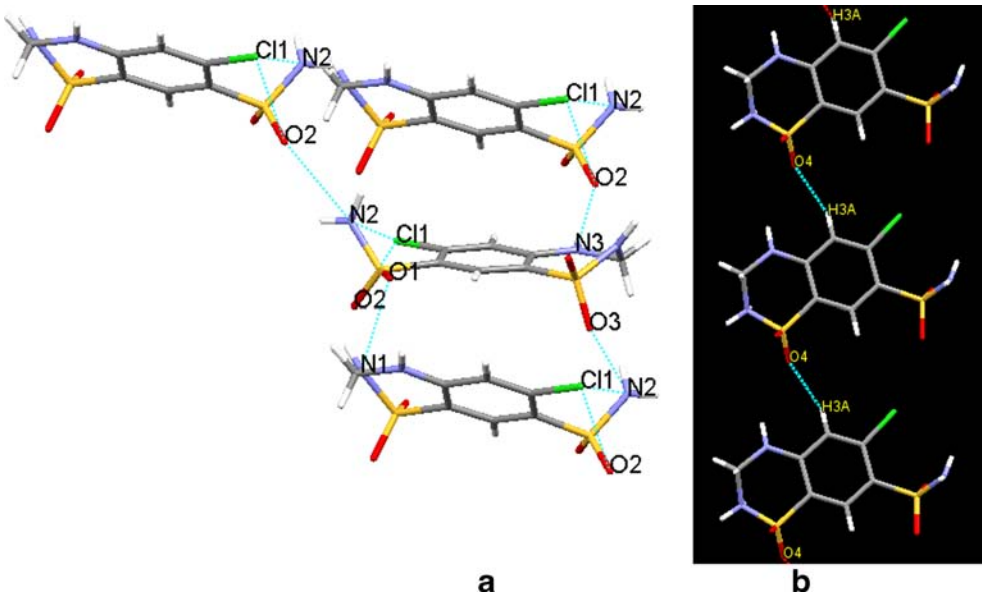

Fig. 2 (**a**) Hydrogen bonds in HCT-Form I. (**b**) C-H….O interaction among HCT molecules.

In both **1** and **2**, the basic heterosynthon extends through various N–H….O interactions and forms a ladder-like packing pattern (Figure S5).

The distinction between a salt and a co-crystal was obtained from C-O bond distances of the carboxylate group of nicotinic acid (ΔDc-o = 0.014 Å) and picolinic acid (ΔDc-o = 0.036 Å) (Table S2) in HCT-NA and HCT-PIC respectively that pointed towards a proton transfer from acidic counter molecules (–COOH group) to the basic HCT molecule.

Solubility Studies

The equilibrium (thermodynamic) solubility studies were carried out in distilled water to evaluate any enhancement in the aqueous solubility of multi-component crystals in comparison to the free drug. The solubility studies were also performed in phosphate buffer pH 7.4 as most of the drug remains in unionized form at this pH and would mimic the intestinal environment. The solubility in phosphate buffer was determined at various time intervals to compare the solubility behavior of the free drug and its salt forms in the basic media.

A slight increase in the equilibrium solubility in distilled water was exhibited by HCT salts after 24 h (0.79 mg/ml, 1.42 mg/ml and 1.16 mg/ml in HCT, HCT-NA (1) and HCT-PIC (2) respectively). However, the increase in drug solublised was much higher in phosphate buffer (pH 7.5) at all the time intervals (Figure S6). HCT-NA showed a 6 fold increase while HCT-PIC showed 2.7 fold increase (at 10 min), in comparison to the free drug molecule.

The FT-IR scans of solid residues (Figure S7) that remained at the completion of the experiment did not show any change in comparison to the original compounds.

The generalized rule of difference of more than 2 pK_a units of the ionizable group in the active pharmaceutical ingredient (API) and in the acid or base is meant to make the proton transfer energetically favorable which in turn determines the fate of the salt in the aqueous media. In the case of prepared salts, a pKa difference of more than 7 units between the –NH

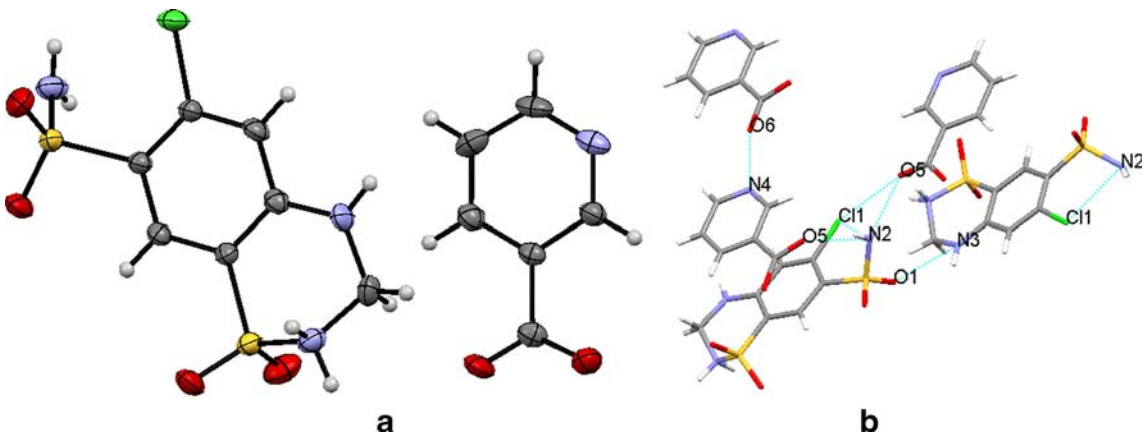

Fig. 3 (**a**) An ORTEP diagram of the asymmetric unit of **I** with 50% thermal ellipsoid. probability and (**b**) hydrogen bonding pattern of **I**.

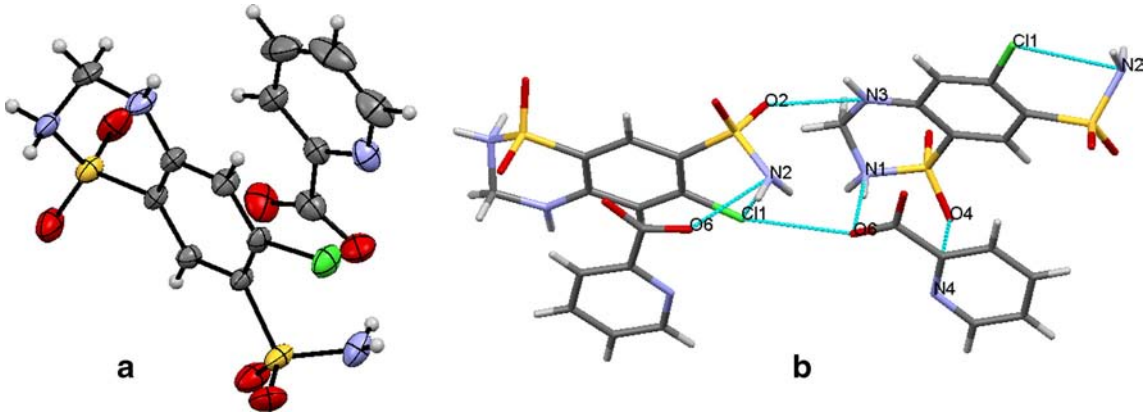

Fig. 4 (**a**) An ORTEP diagram of the asymmetric unit of **2** with 50% thermal ellipsoid probability and (**b**) hydrogen bonding pattern of **2.**

group of HCT and the –COOH functionality of the guest molecules is responsible for a stable complex that does not ionize in the aqueous media.

In Vivo Pharmacodynamic Studies

Antihypertensive Activity Evaluation

The systolic blood pressure of the control rats (group I) (120–130 mmHg) remained constant throughout the study period. However, elevated blood pressure levels were shown by the DOCA induced rats (group II, III and IV) after 2 week of treatment with a mild but significant hypertension. A marked increase in blood pressure levels was observed which reached between 180 and 210 mm Hg after 6 weeks.

After the oral administration of CMC to groups I and II, changes in the systolic blood pressure were recorded and expressed as percentage decrease in the systolic blood pressure. No noteworthy change in the blood pressure levels of rats during the experimental period was observed (Fig. 5).

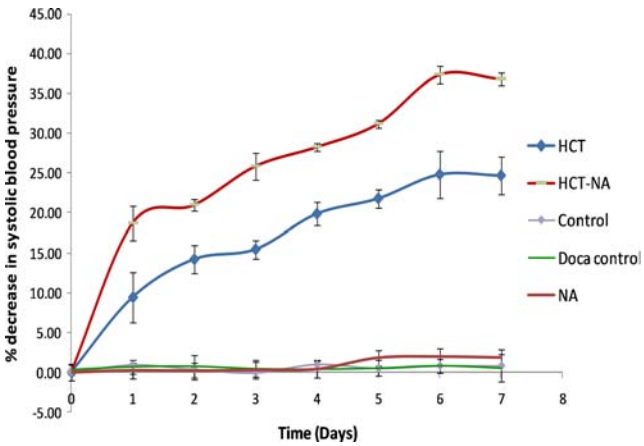

Fig. 5 Antihypertensive activity of HCT-NA in DOCA induced hypertensive rats as compared to the HCT ($n = 6$). Significant decrease in blood pressure as compared to control, DOCA control, NA and HCT groups ($P \leq 0.001$).

However, treatment of groups III and IV with HCT and HCT-NA respectively once daily for a period of 6 days led to significant attenuation of the elevated systolic blood pressure levels of these DOCA salt induced hypertensive rats in comparison to the groups I and II ($P < 0.001$) (Fig. 5). Following the dose treatment, the maximum decrease of systolic blood pressure was 24.7±2.4% in pure drug treated rats and 36.8±0.8% in the multi-component crystal treated ones after 6 days of treatment. The experimental data was statistically analysed by ANOVA and significant decrease in systolic blood pressure due to HCT-NA as compared to the control, DOCA control and the pure drug was observed ($P \leq 0.001$).

The enhanced antihypertensive activity of the multi-component crystal is attributed to the increased dissolution rate of the drug when bonded to the nicotinic acid and thus increased availability at the site of absorption. Many examples are cited in literature where each component of the drug salt *i.e.* the active moeity and the counter ion can exert independently their own pharmacological effect and, in turn potentiate the therapeutic effect. For example in case of drug salts, bamethan nicotinate and xanthinol niacinate, nicotinic acid acts as a peripheral vasodilator and elevates the vasolodilatory effect of the API.

In the present study, nicotinic acid alone did not significantly decrease the blood pressure of the hypertensive rats. However, it is proposed that chronic use of nicotinic acid which is a peripheral vasodilator may decrease the elevated blood pressure and synergise the antihypertensive effect of hydrochlorothiazide.

Conclusively, the pharmacodynamic activity of **1** in rats demonstrated the role of pharmaceutical multi-component crystals in bioavailability enhancement of poorly water soluble HCT with the possible antihyperlipidemic effect of nicotinic acid as an added advantage.

Now, improved dissolution rate and pharmacodynamic activity inspired us to evaluate the toxicological profile of the prepared multi-component crystal, which is essential in the

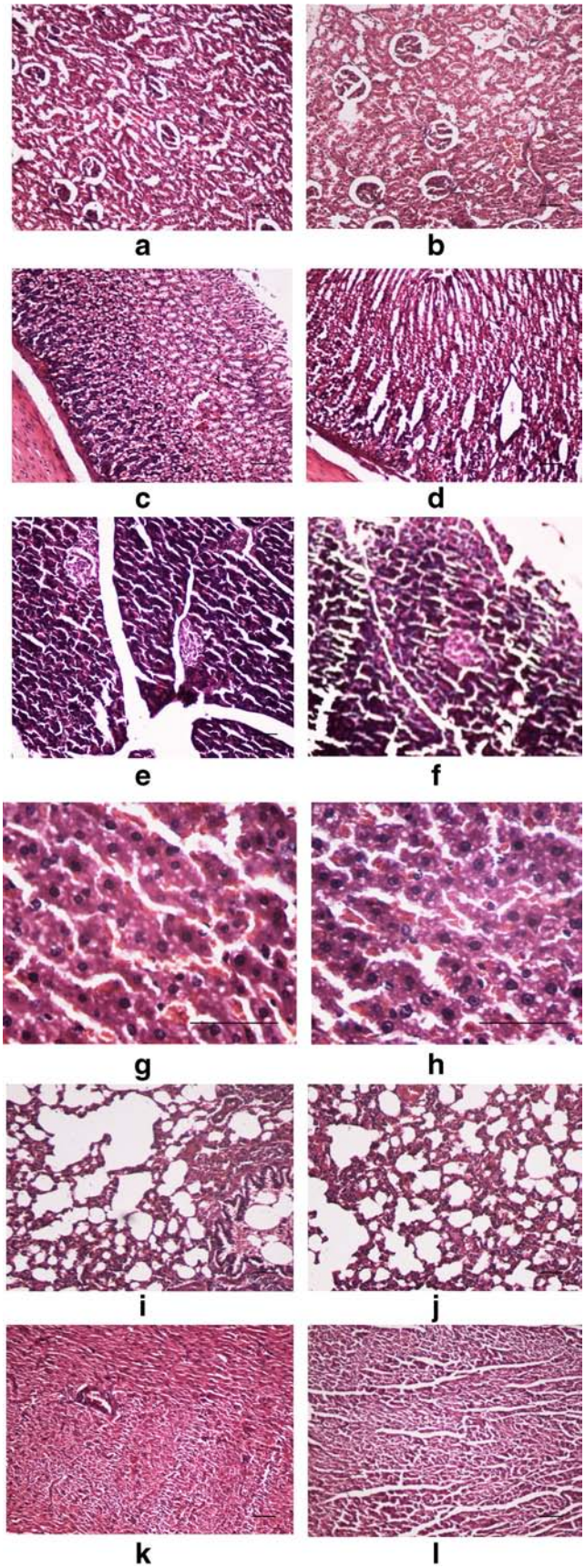

Fig. 6 The microscopic pictures showing pathological changes at determined LD50 values (2,000 mg/Kg) of HCT and HCT- NA (1). The bar in the images represents 10 μm. (**a**) HCT Kidney (100X), (**b**) **1** kidney (100X), (**c**) HCT stomach (100X), (**d**) **1** stomach (100X), (**e**) HCT pancreas– 21– (100X), (**f**) **1** pancreas (100X) (**g**) HCT liver (400 X), (**h**) **1** liver (400 X), (**i**) HCT lungs (100X) (**j**) **1** lungs (100X), (**k**) HCT heart (100X), (**l**) **1** heart (100X).

design of formulation to capture the potential of this multi-component crystal.

Acute Toxicity Studies

Following a single oral dose of HCT and **1** equivalent 2,000 mg/kg BW, the observations concerning the changes in body weight, wellness parameters and histopathological findings of rats were recorded.

Body Weight

No significant changes were observed in BW at the determined LD_{50} values (Table S3) for both HCT and **1**.

Wellness Parameters

Skin, fur, eyes, mucous membrane, behavioral pattern, salivation and sleep of the treated as well as the control animals were found to be normal. No sign of toxicity or death was observed in all the animals treated with HCT and **1** at doses equivalent to 630 mg of HCT/Kg BW and 2,000 mg/Kg BW for HCT and HCT-NA. The LD50 of HCT and **1** was thus found to be >2,000 mg/Kg BW as per the aot425 software.

Histopathological Findings

The acute and chronic toxicity studies of hydrochlorothiazide by oral and intravenous routes have been reported earlier. However, histopathology findings are missing in case of acute toxicity studies. The major side effects which have been reported during the chronic toxicity experiments with HCT include ulcers and erosions of the mucosa of the glandular stomach, hyperplasia of the epitheliod cells of the juxtraglomerular apparatus of kidney and patch-like cytoplasmic basophilia of the centrilobular hepatocytes.

Hence, the animals were observed for histopathological changes in the sections of kidney, liver, stomach, pancreas, lungs and heart. All the sections were grossly normal at the tested dose of HCT equivalent to 2,000 mg/kg BW (Fig. 6) except liver. The liver section showed microvesicular fatty changes in case of HCT which were similar in severity as obtained for **1**.

Thus, the histopathological findings support the LD50 values (>2,000 mg equivalent to HCT/kg BW) of **1** calculated using aot425 software.

CONCLUSION

The present work exemplifies the successful application of crystal engineering approach to achieve an optimal crystal phase of a poor water soluble active pharmaceutical ingredient, HCT. Out of the two multi-component crystals of HCT (HCT-NA and HCT-PIC) HCT-NA was found to be relatively more soluble with a 6 times higher drug dissolution achieved at 10 min and also showed improved antihypertensive activity in terms of percentage decrease in systolic blood pressure (36.8±0.8%) in DOCA induced hypertensive rats. HCT-NA were found to be equally safe as HCT which is exhibited by its LD50 values. The histopathological evidence gained through the examination of stomach, liver and kidney also confirm the safety of this multi-component crystal. It may thus be concluded that HCT-NA shows great potential not only in terms of improved antihypertensive efficacy but also safety, thus making it suitable candidate for formulation development.

ACKNOWLEDGMENTS AND DISCLOSURES

Swati Bhandari and Sadhika Khullar are grateful to Indian Council of Medical Research and Council of Scientific and Industrial Research, New Delhi, India respectively, for their research fellowships. The X-ray facility at IISER, Mohali is gratefully acknowledged. The authors show no conflict of interest.

REFERENCES

1. Lipinski CA. Experimental and computational approaches to estimate solubility and permeability in drug discovery and development settings. Adv Drug Del Rev. 1997;23:3–25.
2. Miroshnyk SM, Sandler N. Pharmaceutical co-crystals–an opportunity for drug product enhancement. Exp Opin Drug Deliv. 2009;6: 333–41.
3. Sandburg A, Abrahamsson B, Sjogren J. Influence of dissolution rate on the extent and rate of bioavailability of metoprolol. Int J Pharm. 1991;68:167–77.
4. Meyer MC, Straughn AB, Mhatre RM, Shah VP, Williams RL, Lesko LJ. The relative bioavailability and in vivo–in vitro correlations for four marketed carbamazepine tablets. Pharm Res. 1998;15: 1787–91.
5. Dressman JB, Amidgon GL, Reppas C, Shah VP. Dissolution testing as a prognostic tool for oraldrug absorption: Immediate release dosage forms. Pharm Res. 1998;15:11–22.
6. Horter D, Dressman JB. Influence of physico-chemical properties on dissolution of drugs in the gastrointestinal tract. Adv Drug Deliv Rev. 2001;46:75–87.
7. Pudipeddi M, Serajuddin ATM, Grant DJW, Stahl PH.. Solubility and dissolution of weak acids, bases and salts. In: Stahl PH, Wermuth CG, editors. Handbook of pharmaceuticalsalts: properties, selection and use. Verlag Helvetica Chemica Acta, Switzerland and Wiley VCH Verlag GmbH and CO,Weinheim.2008; p19–38.
8. Pires MAS, Santos RAS, Sinisterra RD. Pharmaceutical composition of hydrochlorothiazide:β-Cyclodextrin: preparation by Three different methods, physico-chemical characterization and *In vivo* diuretic activity evaluation. Molecules. 2011;16:4482–99.
9. Vishweshwar P, McMohan JA, Bis JA, Zaworotko MJ. Pharmaceutical cocrystals. J Pharm Sci. 2006;95:499–516.
10. Hancock BC, Parks M. What is the true solubility advantage for amorphous pharmaceuticals? Pharm Res. 2000;17:397–404.
11. Chadha R, Bhandari S, Arora P, Chhikara R. Characterization, quantification and stability of differently prepared amorphous forms of some oral hypoglycaemic agents. Pharm Dev Tech. 2013;18(2): 504–14.
12. Hilfiker R. editor.Polymorphism in the pharmaceutical industry. Weinheim: Wiley-VCH Verlag GmbH and Co. KGaA; 2006.
13. Morissette SL, Almarsson O, Peterson ML, Remenar JF, Read MJ, Lemmo AV, *et al.* High-throughput crystallization: polymorphs, salts, co-crystals and solvates of pharmaceutical solids. Adv Drug Del Rev. 2004;56:275–300.
14. TSRL Inc. BCS (Biopharmaceutics Classification System). http://69.20.123.154/services/bcs/results.cfm Accessed 15 Dec 2011.
15. Dupont L, Dideberg O. Structure cristalline de l'hydrochlorothiazide, $C_7H_8ClN_3O_4S_2$. Acta Crystallogr. 1972;B28:2340–7.
16. Florence A, Johnston A, Fernandes P, Shankland K, Stevens HNE, Osmundsena S, *et al.* Powder study of hydrochlorothiazide form II. Acta Crystallogr Sect E. 2005;E61:2798–800.
17. Johnston A, Florence AJ, Shankland N, Kennedy AR, Shankland K, Price SL. Crystallization and crystal energy landscape of hydrochlorothiazide. Cryst Growth Des. 2007;7:705–12.
18. Amarsson Ö, Hickey MB, Peterson M, Zaworotko MJ, Moulton B, Rodriguez-Hornedo N, Pharmaceutical co-crystal composition of drugs such as carbamazepine, celecoxib, olanzapine, itraconazole, topiramate, modafinil, 5-fluorouracil, hydrochlorothiazide, acetaminophen, aspirin, flurbiprofen, phenytoin and ibuprofen. US 2007/0059356.
19. OECD, OECD guidelines for the testing of chemicals.2008.Test number 425. Acute oral toxicity–up-and-down-procedure (UDP).
20. *APEX2*, *SADABS and SAINT*; Bruker AXS inc: Madison, WI, USA, 2008.
21. Sheldrick GM. A short history of SHELX. Acta Crystallogr. 2008;A64:112.
22. Macrae CF, Bruno IJ, Chisholm JA, Edginton PR, McCabe P, Pidocck E, *et al.* Mercury CSD 2.0-New Features for the Visualization and Investigation of Crystal Structures. J Appl Cryst. 2008;41:266.
23. Spek AL. Structure validation in chemical crystallography. *PLATON, Version 1.62*, University of Utrecht, 1999.
24. Childs SL, Stahly GP, Park A. The salt-cocrystal continuum: the influence of crystal structure on ionization state. Mol Pharm. 2007;4: 323–38.